Ship-Based Sun Photometer Measurements Using Microtops Sun Photometers

JOHN N. PORTER

School of Ocean and Earth Science and Technology, University of Hawaii, Honolulu, Hawaii

MARK MILLER

Department of Applied Science, Brookhaven National Laboratory, Upton, New York

CHRISTOPHE PIETRAS

SAIC-General Sciences Corporation, NASA Goddard Space Flight Center, Greenbelt, Maryland

CRAIG MOTELL

School of Ocean and Earth Science and Technology, University of Hawaii, Honolulu, Hawaii

(Manuscript received 13 May 1999, in final form 24 August 2000)

ABSTRACT

The use of hand-held Microtops II sun photometers (built by Solar Light Inc.) on ship platforms is discussed. Their calibration, filter stability, and temperature effects are also described. It is found that under rough conditions, the ship motion causes the largest error, which can result in a bias toward higher optical depths. In order to minimize this bias, a large number of sun photometer measurements (~25) should be taken in a short period of time, and the higher values should be discarded. Under rough ocean conditions, it is also best to shorten the Microtops sun photometer sampling period (less than 5 s) and save only a single value (no averaging) and remove the high optical depths in postprocessing. It is found that the Microtops should be turned off frequently to correct for zero drift caused by temperature effects. Calibration is maintained by routine Langley plot calibrations at the Mauna Loa Observatory for each unit or through cross calibration.

1. Introduction

Aerosol optical depth measurements have been made for many years with two general techniques. One approach uses a narrow field of view radiometer (Volz type) pointed directly at the sun (Volz 1959, 1974; Shaw 1983). This approach is generally considered more accurate but has the added complexity that the sensor must be pointed directly at the sun (with 1°–3° field of view). A second approach uses a shadow band radiometer (Harrison et al. 1994) that measures the total and diffuse radiation from which the direct radiation is derived.

For years, hand-held Volz-type sun photometers with narrow field-of-view sensors have been a popular option, as they can be manually pointed at the sun and are rather inexpensive. They can also be used on ships where most types of automated sun photometers have problems. The hand-held Microtops II sun photometer (referred to here as Microtops sun photometer) is a Volz-type sun photometer, manufactured by Solar Light Inc., which is used by many investigators throughout the world. One such group of investigators is the National Aeronautics and Space Administration's (NASA) Sensor Intercomparison and Merger for Biological and Interdisciplinary Ocean Studies (SIMBIOS) program, which has purchased and maintains numerous Microtops sun photometers for use on diverse ship cruises. The goal of the SIMBIOS measurement program is to obtain high-quality optical measurements for the purpose of validating satellite biological algorithms.

The popularity of Microtops sun photometers is due to their ease of use, portability, and relatively low cost. The instrument has five wavelengths that can be chosen on the basis of the interference filter installed. Depending on the filter combination, the instrument is designed to measure aerosol optical depths, column ozone concentrations, and column water vapor concentrations. The system uses photodiode detectors coupled with amplifiers and A/D converters. The collimators are mounted in a cast aluminum block with a full field of view

Corresponding author address: John Porter, School of Ocean, Earth Science and Technology, University of Hawaii, 2525 Correa Road, Honolulu, HI 96822.
E-mail: jporter@soest.hawii.edu

of 2.5°. The Microtops sun photometer has built-in pressure and temperature sensors and allows for a GPS connection to obtain the position and time. A built-in microprocessor calculates the aerosol optical depths and the ozone or water vapor in real time and displays these values on an LCD screen. The Microtops sun photometer is pointed toward the sun by aligning the sun in a cross-hair screen. The user can adjust the sampling time and the number of values used for the average value saved. Further information on the Microtops sun photometer can be found in Morys et al. (1996). This report is a summary of our experience using the Microtops sun photometer to make aerosol optical depth measurements from ships. Suggestions are given for their use, calibration, and data processing.

2. Accuracy of sun photometer measurements

Much of the earth's remote marine atmosphere aerosol optical depths range from 0.03 to 0.05. For these regions, an error of 0.01 in the measured optical depth is substantial and can affect the ability to derive aerosol size information from the wavelength dependence of the aerosol optical depths. Cited uncertainties in sun photometer calibration typically range between 0.005 and 0.02 (Shaw 1983; Harrison et al. 1994; Ehsani et al. 1998; Holben et al. 1998). These uncertainties are primarily due to inaccurate calibration, error in correction of molecular scatter and absorption, and faulty instrumentation (dirty optics included). Sun photometers are typically calibrated by using the Langley plot approach (Reagan et al. 1986; Russell et al. 1993; Schmid and Wehrli 1995), which is based on the Beers law:

$$I = I_o\left(\frac{d_m}{d}\right)^2 e^{-(\tau_a m_a + \tau_m m_m + \tau_{O_3} m_{O_3} + \tau_t m_t)}, \quad (1)$$

where I and I_o are the direct radiation at the top and bottom of the atmosphere, respectively; τ_a and m_a are the aerosol optical depth and air mass, respectively; τ_m and m_m are the molecular optical depth and air mass, respectively; τ_{O_3} and m_{O_3} are the ozone optical depth and air mass, respectively; and τ_t and m_t are the trace gas optical depth and air mass, respectively. Following Paltridge and Platt (1977), the ratio of mean sun–earth distance to the daily distance is

$$\frac{d_m}{d} = \{1 - 0.01673 \cos[0.017201(\mathrm{doy} - 4)]\}^{-1}, \quad (2)$$

where doy is the day of the year. Rather than use the solar zenith angles provided by the Microtops, we have used those calculated by the sunangle software, which is available from Susdesign on the Internet. Below 60°, the molecular air mass, m_m, can be calculated by the secant of the solar zenith angle. Above 60°, the air mass should be corrected for the curvature of the earth and the vertical distribution of molecules (Lenoble 1993; Kasten and Young 1989) and can be calculated by

$$m_m = [\sin(\gamma) + \alpha(\gamma + b)^{-c}]^{-1}, \quad (3)$$

where γ = solar zenith angle, $\alpha = 0.505\,72$, $b = 6.079\,95$, and $c = 1.6364$. In order to calculate the aerosol and trace gas air mass, their vertical distributions are needed. Unfortunately, this is rarely available, so we assume their air masses follow the molecular air masses for normal conditions (no major volcanic eruptions). The ozone has a strong peak in the stratosphere near 22 km and is therefore significantly different from the molecular vertical distribution. Employing the calculations done by Thomason et al. (1983), we have fit a polynomial to calculate the ozone air mass as a deviation from the Kasten and Young (1989) molecular air mass given in Eq. (3):

$$m_{O_3} = m_m + \Delta m, \quad (4)$$

where $\Delta m = -0.011m_m + 0.027m_m^2 - 0.0161m_m^3$.

Assuming the detector is linear, the sensor voltage (V and V_o) can be substituted into Eq. (1), and after rearranging, we obtain

$$(\ln V + \tau_{O_3} m_{O_3}) = -m_m(\tau_a + \tau_m + \tau_t) + \ln V_o', \quad (5)$$

where $V_o' = V_o(d/d_m)^2$. In Eq. (5), V_o is the annual average extraterrestrial constant (corrected for the sun–earth distance), and V_o' is the extraterrestrial constant one would obtain from a Langley plot calibration on any particular day. Equation (5) has the form of a straight line (y = slope $x + b$), where the y axis values are ($\ln V + \tau_{O_3} m_{O_3}$), the x axis values are the molecular air mass (m_m), the slope of the line is $-(\tau_a + \tau_m + \tau_t)$, and the zero intercept value is $\ln V_o'$. By making measurements of the direct solar beam throughout the sunrise and plotting them as ($\ln V + \tau_{O_3} m_{O_3}$) versus m_m, it is possible to obtain a straight line, which has a slope equal to the optical depth. By extending the straight line back to zero air mass the extraterrestrial constant, $\ln V_o'$ is obtained, which is what the instrument would measure if it was above the atmosphere on that day. Once $\ln V_o'$ is determined, the optical depth can be determined from a single voltage measurement by

$$\tau = \left(\frac{1}{m_m}\right)[-\ln(V) + \ln(V_o') - \tau_{O_3} m_{O_3}], \quad (6)$$

where $V_o' = V_o(d/d_m)^2$ and $\tau_a = \tau - \tau_m - \tau_t$. In carrying out the Langley plot calibration to obtain V_o', it is assumed that the optical depth remains constant during the measurements. The Mauna Loa Observatory (MLO) on the island of Hawaii is often chosen for these efforts (Shaw 1982, 1983; Holben et al. 1998), as it is above the trade wind inversion and has fairly low and stable aerosol optical depths throughout much of the year. At this site, measurements typically take less than 2 h to cover the air mass range from 5 to 2, which is sufficient for a good calibration. The fact that the calibrations are made over a relatively short 2-h time period helps in the assumption that the aerosol will remain constant.

An example of this Langley plot effort for a Micro-

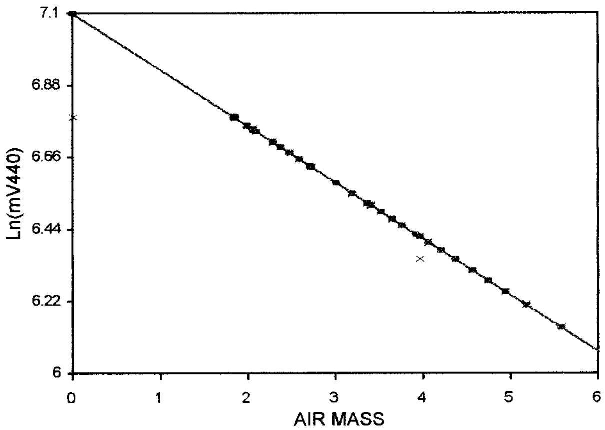

FIG. 1. Langley plot (440 nm) collected at the MLO on 27 Feb 1998.

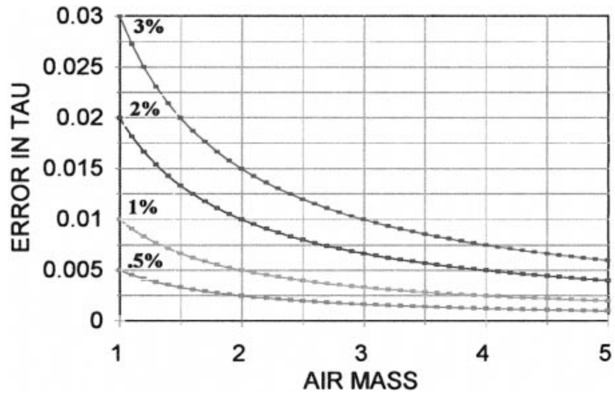

FIG. 2. The error in the derived total optical depth as a function of air mass and for different percentage errors in ($\Delta V_o/V_o - \Delta V/V$). The errors occur at small air mass.

tops sun photometer is shown in Fig. 1. For this day, it can be seen that the measurements fit a straight line well and the $\ln V_o'$ appears to be well determined. Any error in pointing toward the sun will cause a bias towards higher optical depths. Therefore, our approach to process Langley plots is to 1) fit a line to the data, 2) throw away any data points that are more than 0.1% below the line, and 3) refit the line. This process is continued until all measurements are within 0.1% of the line or higher. This iterative approach minimizes manual pointing errors. In Fig. 1, it can be seen that this approach removes the low measurements at air mass 3.9, which are likely due to poor pointing.

Taking the derivative of Eq. (6), the error in aerosol optical depth is given by

$$\Delta\tau_a = \frac{1}{m_m}\left[-\tau\Delta m_m + \frac{\Delta V_o'}{V_o'} - \frac{\Delta V}{V} - \tau_{O_3}\Delta m_{O_3} - m_{O_3}\Delta\tau_{O_3}\right] + \Delta\tau_m + \Delta\tau_t \qquad (7)$$

where $\tau = \tau_a + \tau_m + \tau_t$, which is similar to a form given by Reagan et al. (1986). The first term on the right describes the error due to uncertainty in the molecular air mass calculation, which includes the uncertainty in the aerosol and trace gas air mass. The second term is the uncertainty in the calibration (V_o'). The third term describes an error in the actual measurement that could be caused by improper pointing at the sun, dirty optics, or unstable electronics (temperature dependence, etc). The next two terms are due to error in the ozone air mass and optical depth. The last two terms are due to error in the calculation of molecular and trace gas optical depths.

All of the error equations are affected by the air mass so that as air mass increases, the error decreases (holding all other terms constant). This point can be illustrated on Langley plots, such as Fig. 1. If two points on the plot [$\ln(V_o')$ and $\ln(V)$], are close together (i.e., small air mass), then errors in either V_o' or V will affect the slope more than if the two points are far apart (i.e., large air mass). This effect is illustrated in Fig. 2, which shows the error in optical depth one would obtain for a given error in V_o' or V as a function of air mass. For this illustration, the other error terms are set to zero ($\Delta m_m = \Delta m_{O_3} = \Delta\tau_{O_3} = \Delta\tau_m = \Delta\tau_t = 0$). Assuming there is no error in the measurement ($\Delta V = 0$), a 0.5% error in the calibration of V_o' results in an error of 0.005 in optical depth at low air mass. Conversely, a 0.5% error in the measurement gives a 0.005 error in optical depth at low air mass, assuming the calibration of V_o' was perfect.

We would like to make aerosol optical depth measurements with an accuracy of 0.005. With this accuracy goal, the error in calibration of the sun photometer (V_o') should be less than $\pm0.5\%$ for measurements at air mass one (sun directly overhead). At larger air mass, the errors in the aerosol optical depth decrease. This sensitivity with air mass is of concern, since most of the satellites, which are used to derive aerosol optical depths (AVHRR, SeaWifs, EOS-AM1), make measurements near noon solar time (between 0100 and 1400 local time) when low air mass values can occur.

The V_o taken from selected Langley plots for the Microtops units (3694 and 3774) is shown in Fig. 3. Langley plots were taken mostly at the MLO, Hawaii, but some were also taken from Haleakala, Maui. Figure 3 is from the Langley plots for which more than 90% of the measurements fit the line (to within 0.1%). The V_o standard deviation for the 380, 440, 500, 675, 870, and 1020 channels was 0.9%, 0.32%, 0.44%, 0.28%, 0.83%, and 1.5%, respectively. Based on these measurements, we conclude that the calibration has remained constant throughout the year for these particular Microtops sun photometers.

3. Error due to electronic failure, filters, pressure, temperature, and pointing

Besides calibration issues, error in the sun photometer measurements can be caused by changes in electronics,

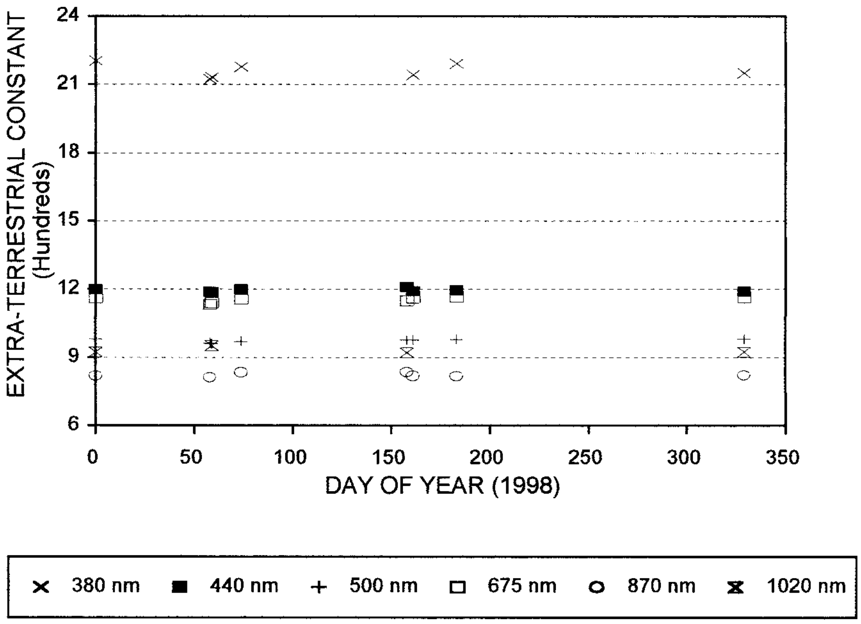

FIG. 3. Time series of extraterrestrial constants (V_o') for two Microtops sunphotometers.

filter degradation, temperature effects, and poor pointing at the sun ($\Delta V/V$ term). Faulty electronics is a potential problem that is not always easy to detect. In the past, we have found that a leaky capacitor (present in one of our Microtops) lowered the power and created erratic behavior for the shorter wavelengths, where more gain is required. A weak battery may also cause similar problems, but the Microtops sun photometer has a battery sensor so that presumably this may not be such a serious problem. One way to minimize this problem is to turn the sun photometer off and on before each measurement. This allows the Microtops to make a reference dark measurement within a short time from the actual measurement. One can also get some idea of the stability by taking numerous measurements with the lid covered. The voltage on all five channels should be less than ± 0.03 mV, and the variability will give some idea of the noise present in the photometer.

Our Microtops sun photometers have been used in many temperatures and humiditys over the past year on Hawaii Ocean Time Series (HOT) monthly ship cruises, Mauna Loa and Haleakala calibrations, and aircraft measurements. Filter degradation under these conditions is of concern. The Microtops sun photometers use ion-deposited Barr filters, which are supposed to have an unlimited lifetime. Although we only have a limited time sample, the calibrations shown in Fig. 3 show no sign of filter decay. On the other hand, one of our Microtops is experiencing significant decay for the 440-nm filter. Others have experienced similar results (B. Holben 1997, personal communication), suggesting that at least one batch of bad Barr filters exists.

The temperature affects the dark counts and possibly the gain of the Microtops sunphotometers. An example of the temperature effect is shown in Figs. 4a and 4b. For this test the Microtops was heated and cooled to reach the temperatures shown. The measurements were made in the saddle between Mauna Loa and Mauna Kea on the big island of Hawaii (1 March 1989) and took approximately 45 min to complete. Here, it is assumed that the aerosol optical depth remained approximately constant during the measurements, which is consistent with visual observation and the fact that the optical depths follow the temperature down after the hour 21.5. Clear temperature dependence is shown here for the 500-nm channel. These measurements were made without turning the instrument off so that only one dark measurement was made at the beginning of the experiment. Figure 5 shows a subsequent temperature test (at Mauna Loa, 26 November 1998) where the Microtops was turned off and on before each measurement. Simultaneous measurements were made with another Microtops instrument. The temperature of unit 3756 remained approximately constant while the temperature of Microtops unit 3774 was cooled and heated from $\sim 0°$ to $-40°$C. During the same time period, the aerosol optical depths from the two units remained approximately constant. This suggests turning the Microtops off and on before each measurement properly corrected for the temperature effects. In deriving these aerosol optical depths, the average V_o (Fig. 3) was used, and molecular scatter was removed based on the instrument pressure.

Error in the molecular optical depth directly affects the aerosol optical depth [Eq. (7)]. The molecular optical depths for the Microtops 380, 440, 500, 675, 870, 935, and 1020 nm channels at 1013 mb are 0.449, 0.241, 0.144, 0.0424, 0.0152, 0.0113, 0.008 03, respectively.

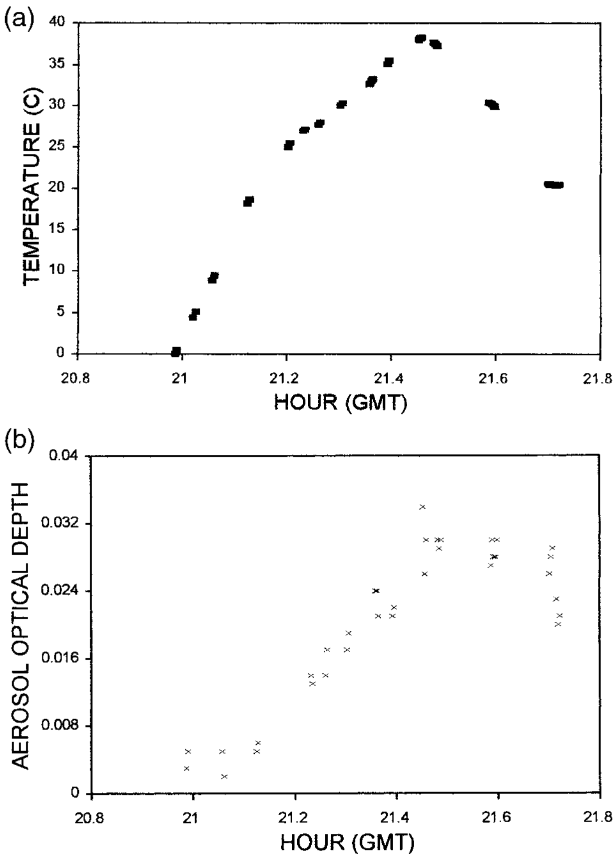

FIG. 4. Microtops temperature dependence if dark measurements are not made. (a) Temperature of the Microtops. (b) Aerosol optical depth (500 nm) obtained from the Microtops.

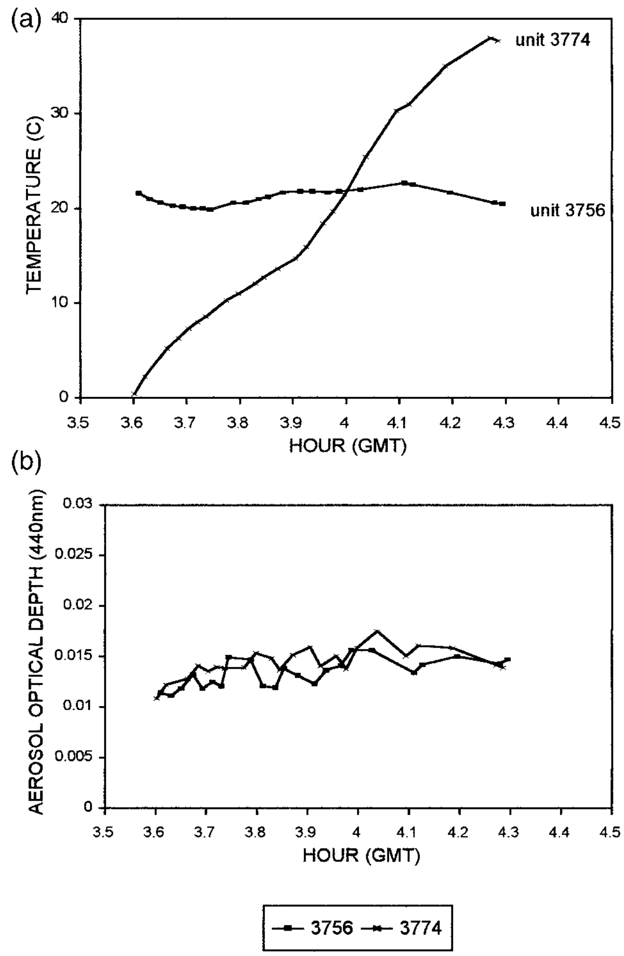

FIG. 5. (a) Temperature time series for Microtops sun photometer units 3756 and 3774. (b) Time series of aerosol optical depths for the same units.

These values were calculated from the spectral response of each filter [see Eq. (9) below] based on the factory FWHM (full width half maximum) filter values. These molecular optical depths decrease with height by P/P_o where P_o is the surface pressure (1013 hPa). The Microtops sun photometers can be ordered with built-in pressure sensors. We have compared four Microtops with a NIST traceable Vaisala PTB220 class A pressure sensor, which is accurate to better than ± 0.1 hPa from 1050 to 500 hPa. The four Microtops were within 2–3 mb high, suggesting a bias of ~ 2.5 mb and a variability of ~ 1.5 mb. If we assume the error is ± 3 mb, this corresponds to 0.3% error for pressure values 1013 mb, which equals an uncertainty in the molecular optical depth at 380 nm of 0.0013 and lower at longer wavelengths.

Pointing the hand-held sun photometer at the sun is one of the major sources of error in making sun photometer measurements at sea. This problem is illustrated in Fig. 6, which shows aerosol optical depth measurements made on a HOT ship cruise north of Oahu. On day 221, the winds were typical trades with swells moving in mainly one direction. The Microtops operator is able to point at the sun fairly accurately. On day 222

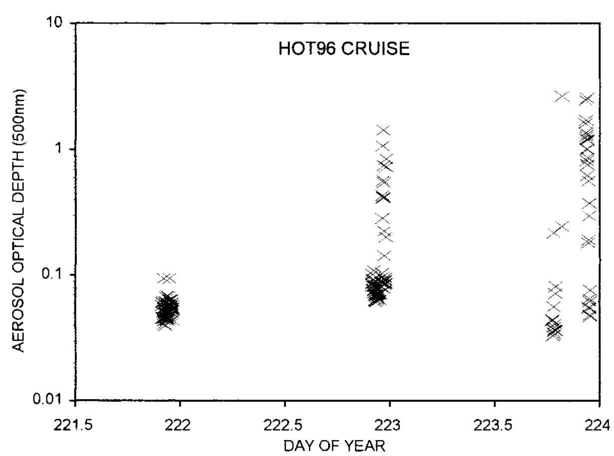

FIG. 6. Time series of aerosol optical depths during HOT96 cruise north of Hawaii (9–12 Aug 1999).

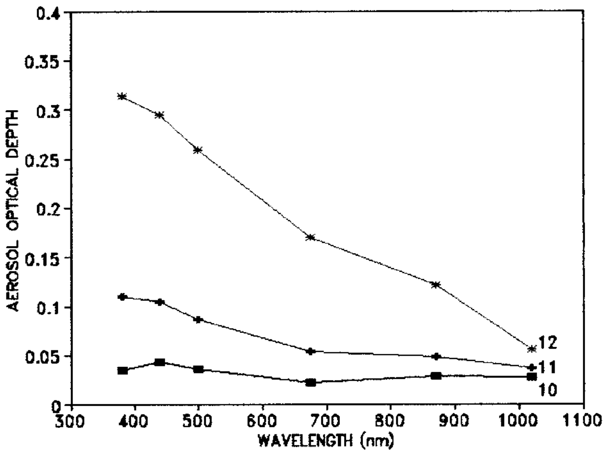

FIG. 7. Spectral dependence of aerosol optical depths measured on 10–12 Jan 1998 on HOT89 cruise.

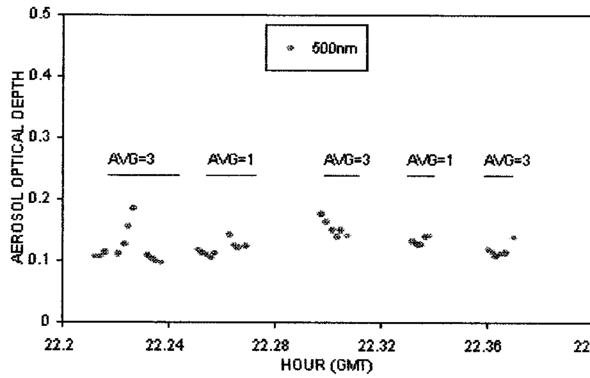

FIG. 8. Measurements of optical depth using different averaging times.

and 223 the operator began to have problems possibly as a result of crossed swells as a tropical depression was approaching. It can be seen that when many measurements are made, a cluster of data exists near the bottom with a tail to higher optical depths as errors in pointing cause a bias to larger optical depths. When fewer measurements are made (e.g., day 223.9), then it is not clear which data are correct. Since we have low measurements on previous days and on the same day, it is likely that only the lowest data (below 0.1) are good. Before removing the larger values, one should first plot the data as a short time series to see if the large variations are part of a systematic trend. Poor pointing errors will appear as noise, while real aerosol variations will have a more systematic behavior. This visual inspection and manual removal of bad data needs to be carried out for each channel of the Microtops. While it is possible that one will delete good data with this approach, it will also remove a large amount of bad data, which is the lesser of two evils.

One alternative to reduce the pointing problem on the ship is to reduce the averaging number to one. This way only a single highest value (lowest optical depths) will be saved each time. Figure 8 shows a test where the total optical depths are measured using different averaging values. Measurements were made on a beach with varying salt spray amounts from breaking waves. The difference in averaging does not appear to cause any significant change in the average value or the variability. Based on this test it would appear that for use on a ship, the averaging should be set to 1, and the sampling period can be set down to 5 s or less. This will improve the chances that at least some of the measurements will be correct and speed the sampling. As discussed above, postprocessing to remove the high values is still needed.

4. Correction for ozone, water vapor, and trace gas optical depth

Although the wavelengths of the Microtops sun photometer are chosen to avoid major atmospheric absorption regions, some amount of absorption is still present. Based on specifications obtained from the manufacturer, we have calculated the weighted optical depths of ozone, water vapor, and trace gasses for each channel of the Microtops. These are given in Tables 2 and 3. Calculations were based on atmospheric transmittances from the MODTRAN code, and the filter spectral response was modeled using the filter FWHM at 1-nm intervals using

$$\overline{T} = \frac{\sum T_\lambda S_\lambda F_{r,\lambda}}{\sum S_\lambda F_{r,\lambda}} \tag{8}$$

where $\overline{T}$ = weighted atmospheric transmittance, T_λ = monochromatic atmospheric transmittance, $F_{r,\lambda}$ = monochromatic filter response, and S_λ = solar spectral response. Water vapor only has a significant absorption in the 1020-nm wavelength, and the water vapor optical depth ranges from 0.002 to 0.008 for midlalitude winter to tropical atmospheres. The water vapor optical depth in the 1020 nm channel can be calculated from

$$\tau_{wv} = (H_2O\ \mathrm{mm})0.001\,96 + 0.000\,192, \tag{9}$$

which is based on a fit to MODTRAN calculations using Eq. (8). Molecular optical depths were 0.450, 0.242, 0.144, 0.043, 0.015, 0.0113, and 0.008 at 380, 440, 500, 675, 870, 935.8, and 1020 nm, respectively.

5. Calibration of the SIMBIOS Microtops sun photometers

The SIMBIOS program maintains numerous Microtops sun photometers that are used by investigators in diverse ship cruises. It is generally not feasible to perform high-altitude Langley plot calibration for each of these sun photometers because of time and budget constraints. An alternative is to perform a calibration transfer from a calibrated sun photometer. This approach is used routinely by the AERONET network, which maintains two sun photometers at the MLO and occasionally brings one back to NASA/Goddard Space Flight Center to cross-calibrate other sun photometers (Holben et al.

TABLE 1. V_O of the Microtops #3773 obtained at GSFC by intercalibration with the Cimel #37 (August) and #27 (next month). The standard deviation (STD) and STD % are also shown.

Date	440 nm	500 nm	675 nm	870 nm	940 nm
20 Aug 1998	1238 ± 7	988 ± 4	1219 ± 5	825 ± 3	1429 ± 8
21 Aug 1998	1244 ± 8	988 ± 12	1218 ± 10	824 ± 7	1421 ± 9
24 Nov 1998	1222 ± 3	976 ± 2	1192 ± 3	823 ± 3	1411 ± 5
9 Jun 1999	1240 ± 4	988 ± 4	1202 ± 3	826 ± 2	1406 ± 8
MEAN	1236	985	1208	825	1417
STD	10	6	13	1	10
STD %	0.78	0.61	1.08	0.16	0.73

1998). The SIMBIOS program uses the same method to calibrate their Microtops sun photometers, using a calibrated Cimel sun photometer as the standard. The Cimel is calibrated at the high-altitude National Oceanic and Atmosphere Administration (NOAA) MLO (Hawaii) by applying the Langley plot method (Holben et al. 1998).

The calibration transfer consists of taking simultaneous direct sun measurements with the Microtops and the Cimel sun photometers during a clear day. The ratio of the raw measurements can be expressed as

$$\frac{V_i^{\text{cimel}}}{V_i^{\text{mtops}}} = \frac{V_{0i}'^{\text{cimel}}}{V_{0i}'^{\text{mtops}}}. \tag{10}$$

Here, i is the channel number of the Microtops and the same channel of the Cimel instrument (same center wavelength). The left side of the ratio is for instantaneous measurements, and the right side is for the extraterrestrial constant. The method can be extended to a different channel if the Rayleigh scattering and ozone absorption is taken into account in the two spectral bands.

Table 1 gives the V_o and standard deviations (for each calibration effort and the long-term average) for one Microtops sun photometer (unit 3773), which was calibrated during August 1998 and June 1999 by comparing with a reference Cimel. The Microtops and Cimel measurements were made nearly simultaneous. The calibration is typically rejected if the standard deviation for a particular day is higher than 1% (one exception is 21 August 1998, which was retained).

6. Aerosol optical depth accuracies

In order to calculate the accuracy of the Microtops sun photometer measurements, we now consider each term in Eq. (7). For these calculations, we assume the total optical depth is 0.52, 0.3, 0.2, 0.11, 0.07, and 0.06 at 380, 440, 500, 675, 870, and 1020 nm, respectively. This corresponds to an aerosol optical depth of close to 0.05 at each wavelength, which is common for marine atmospheres. The first term in Eq. (7), $-\tau\Delta m_m/m_m$, is due to uncertainty in the molecular air mass, which depends on the ability to calculate the air mass and to measure the pressure (air mass varies by P/P_o). Based on the range of air masses computed (using numerical integration) by Kasten and Young (1989) and Thomason et al. (1983), $\Delta m_m/m_m$ can be calculated with an accuracy of $\sim$0.5%. As discussed earlier, the pressure can be measured to better than $\pm$3 hPa, which results in a $\Delta P/P$ error of 0.003 at 1013 hPa. Adding the calculation and pressure uncertainties results in a 0.008 uncertainty factor. Multiplying by the total optical depths given above results in errors of 0.0042, 0.0024, 0.0016, 0.0008, 0.000 56, and 0.000 48 for the $-\tau\Delta m_m/m_m$ term at each wavelength.

The second term in equation 7, $\Delta V_o'/(m_m V_o')$, is due to an error in calibration. Assuming a normal distribution, 95% of the Langley plot calibrations obtained on different days will lie within two standard deviations of the average of the calibrations. The V_o standard deviation for the 380, 440, 500, 675, 870, and 1020 channels were 0.9%, 0.32%, 0.44%, 0.28%, 0.83%, and 1.5%, respectively. Taking two standard deviations and multiplying by $1/\sqrt{7}$ to account for the improvement when averaging many measurements results in uncertainties of 0.0068, 0.0024, 0.0033, 0.0021, 0.0063, and 0.0113 for the $\Delta V_o'/(m_m V_o')$ error term. Seven different Langley plot calibrations were used here. More Langley plot calibrations would reduce the uncertainty, but at some point, the improvement would be limited by the assumption that the error is truly random, which may not be perfectly correct.

The next term, $\Delta V/(m_m V)$, is mainly due to poor pointing, dirty optics, or electronic noise. Dirty optics is easy to correct, and we assume the operator is capable of fixing this problem. Over land, pointing at the sun is fairly easy. We can get some idea about this error term by comparing a time series of sun photometer measurements at a clean site where the optical depth and therefore the aerosol variability is small. Figure 5b shows a time series of aerosol optical depths taken at the MLO with two sun photometers. The aerosol optical depths trend together and vary with respect to each other by less than $\pm$0.03. Based on this example, we assume a 1 standard deviation error of $\pm$0.0025 in pointing at the sun and noise. Next, we assume 2 standard deviations (0.005) include 95% of error. If 10 measurements are averaged, then the error decreases by $1/\sqrt{10}$, resulting in an error of 0.0016 for the $\Delta V/(m_m V)$ term.

On a moving platform, pointing at the sun is much more difficult, and the pointing error increases depend-

TABLE 2. Weighted ozone optical depths for the Microtops channels. The filter center wavelength and FWHM are also given.

	380 nm	440 nm	500 nm	675 nm	870 nm	1020 nm
Midlat summer	0	0.001	0.0106	0.0135	0	0
Midlat winter	0	0.0013	0.012	0.0154	0	0
Tropical	0	0.0008	0.009	0.0013	0	0
Average	0	0.001	0.0105	0.0134	0	0

ing on the sea roughness. After removing the biased large values, the 1 standard deviation values in our measurements are typically 0.0125. Taking two standard deviations and multiplying by $1/\sqrt{10}$ (for an average of 10 measurements) results in an error of 0.008 for the $\Delta V/(m_m V)$ term.

The next error term in Eq. 7, $\tau_{O_3}\Delta m_{O_3}/m_m$, describes the error due to ozone optical depth. From Table 2, the average ozone optical depths are 0, 0.001, 0.0105, 0.0134, 0, and 0 for the 6 wavelengths. The largest ozone absorption occurs in the 675 nm channel. At a small air mass, the error in the ozone air mass calculation ($\Delta m_{O_3}/m_{O_3}$) is equal to the error in calculating the molecular air mass (0.005), as discussed above. Multiplying by τ_{o_3} (0.0134) results in 0.000 067, which is negligible. For larger air masses, Eq. (4) can be used to calculate m_{O_3}. Based on the cases shown in Thomason et al. (1983), $\Delta m_{O_3}/m_{O_3}$ is approximately 0.026. As the ozone height can vary, we double the error to 0.052 and multiply by τ_{o_3} (0.0134), which results in an error of 0.0004 which is also negligible.

The next error term, $m_{O_3}\Delta\tau_{O_3}/m_m$, accounts for uncertainty in the ozone optical depth. We assume the average error of $\tau_{O_3} = 0.0134$ (see Table 2 at 675 nm) and can have a 15% uncertainty so that $\tau_{O_3} = 0.002$. At low air mass, the error term $\Delta m_{O_3}\Delta\tau_{O_3}/m_m$ has a value of 0.002, and at higher air mass value, decreases slightly.

The next term, $d\tau_m$, accounts for the error in the molecular optical depth. Tiellet (1990) compared several techniques to derive the molecular optical depth. He found variations due to atmospheric profiles produced 1% variations. He also found the fitting equation given by Hansen and Travis (1974) and Gordon et al. (1980) fit the best calculations to within 0.1% from 350 to 900 nm, with the largest error occurring at the shortest wavelengths. Combining these two uncertainties results in a 1.1% uncertainty. The molecular optical depths for the Microtops 380, 440, 500, 675, 870, and 1020 nm channels at 1013 hPa are 0.449, 0.241, 0.144, 0.0424, 0.0152, and 0.008 03, respectively. This results in a $d\tau_m$ error of 0.005, 0.0026, 0.0016, 0.0005, 0.0002, 0.0001, and 0.000 09.

The final error term in Eq. (7) is the trace gas optical depth ($d\tau_T$) error. From Table 3, the average trace gas optical depths are 0.003, 0.0028, 0.001 35, 0.0007, 0.0005, and 0. Based on the small variability seen in Modtrans for different atmospheres, we assume a 25% in trace gas optical depths resulting in a $d\tau_T$ of 0.000 75, 0.0007, 0.0034, 0.0002, 0.0001, and 0.

Combining each term results in aerosol optical depth errors of ± 0.02, 0.012, 0.01, 0.007, 0.011, and 0.015 avg for our land-based measurements for the different wavelengths. Ship-based aerosol optical errors increase to 0.026, 0.018, 0.016, 0.013, 0.017, and 0.02 avg. For the transfer calibration, we add the uncertainty of the transfer to the existing error. The 1 standard deviation in Table 1 is multiplied by 2 to account for 95% of the variability and by $1/\sqrt{4}$ to account for the error reduction in averaging. Adding this transfer error to the existing error results in aerosol optical depth errors of 0.023, 0.018, 0.021, 0.012, and 0.023 (average 0.019) for land-based measurements. For ship-based measurements, the error increases to 0.029, 0.024, 0.027, 0.019, and 0.028 (average 0.025).

The errors given above refer to the 95% values, but most of the errors will be less. One way to estimate the error is to compare aerosol optical depths measured with two independent sun photometers (each calibrated separately). Figure 5b is one example where the difference between the two is closer to 0.03 at 440 for land-based measurements. Although we do not have identical wavelengths, we have collected many ship-based measurements using two Microtops sun photometers. One has a 875-nm channel, and the other has a 1020-nm channel. When sea salt dominates, the wavelength dependence of the aerosol optical depth is flat so that the aerosol optical depth at 875 and 1020 are very close (i.e., see day 10 in Fig. 7). Based on numerous measurements,

TABLE 3. Weighted trace gas optical depths for the Microtops channels.

	380 nm (379.5 nm) FWHM = 3.8 nm	440 nm (440.7 nm) FWHM = 10.0 nm	500 nm (499.8 nm) FWHM = 10.4 nm	675 nm (674.6 nm) FWHM = 10.8 nm	870 nm (870.3 nm) FWHM = 10.2 nm	1020 nm (1019.7 nm) FWHM = 10.5 nm
Midlat summer	0.00315	0.0029	0.0014	0.00065	0.00055	0
Midlat winter	0.0029	0.0026	0.0013	0.007	0.006	0
Tropical	0.003	0.0028	0.0014	0.0007	0.0005	0
Average	0.003	0.0028	0.00135	0.0007	0.0005	0

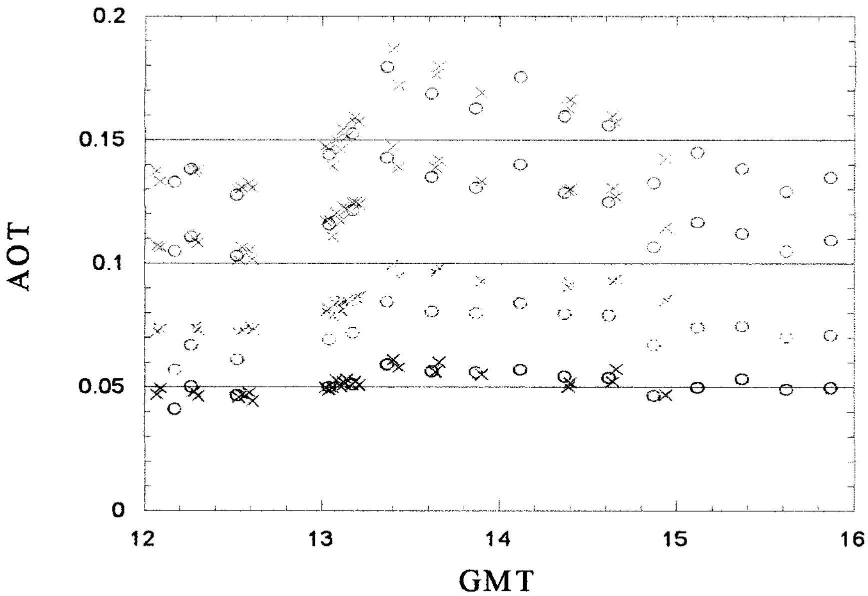

FIG. 9. AOT comparisons between a calibrated Cimel and the Microtops #3773. The Microtops has been calibrated according to the Cimel #37 on 20 Aug 1998, and these measurements were made on 21 Aug 1998.

we find the aerosol optical depths at 875 and 1020 are within 0.01 (or better) for ~90% of the measurements. These few comparisons suggest that the most common error are likely to be less than the error values given above.

7. Measurement discussion

Numerous precautions are needed in making Microtops sun photometer measurements from ships. For open ocean conditions, we suggest setting the averaging to 1 sample and setting the sampling to 32 (less than 5 s sampling). This saves only the lowest optical depth collected during the sampling period. We also suggest collecting 25 sun photometer measurements as quickly as possible. Before each measurement, the Microtops should be turned off and on to allow for dark count correction. The complete 25 measurements will take less than 5 min of time, including turning the unit off and on.

The collected data should be plotted, and large values should be removed if they are not part of a systematic trend. This visual inspection should be done for each channel, and it should not be assumed that removing all bad data points in one channel would remove all bad data in another channel. In this process, we allow for optical depth variability of 20% of the final average value or 0.025 when the optical depths are below 0.08. This approach may slightly bias the data to lower values, but it will remove the unrealistic larger values that would occur if the data were not processed. Exceptions are made when the data shows a systematic trend during the measurement period.

On several instances, we have found condensation to be a problem when the Microtops was stored in air-conditioned rooms prior to making measurements. If this is a problem, the sun photometer should be placed in the sun to warm up to temperatures higher than ambient temperatures prior to making the measurements. The temperature can be monitored to ensure that enough warming has occurred.

The lens of the Microtops should be cleaned prior to each measurement period. For the open ocean, salt is the primary contaminant. Under these conditions, a lens tissue can be wet with clean (filtered, if possible) water and used to remove the salt followed by a dry lens tissue to remove all water drops.

In order to test the Microtops electronics, several dark measurements should be taken with the Microtops lid covered. The volts for each channel should be less than ±0.03 mV. If the voltage is above ±0.03 mV, the instrument will still work, but it must definitely be turned off and on before each measurement. If the problem persists, then the unit should be sent back to the manufacturer for repair.

8. Conclusions

The Microtops sun photometers offer a rather inexpensive and convenient way to measure aerosol optical depths. Their simple design makes them ideal for field experiments, such as ship cruises. They can provide good quality measurements on moving platforms, but specific precautions must be followed. We have found that making measurements on ships requires one to make many measurements and to manually remove the bad measurements. We have also found that their temperature dependence requires one to turn the instrument off and on before each measurement to ensure good dark count correction.

Acknowledgments. The work described here was carried out as part of the NASA SIMBIOS project. We would like to thank Dave Karl, Louie Tupas, Terry Houlihan, and Dale Hebel (members of the Hawaii ocean time series) and Steve Poulous (ship staff), who either made or assisted in making the ship measurements.

REFERENCES

Ehsani, A. R., J. A. Reagan, and W. H. Erxleben, 1998: Design and performance of an automated 10-channel solar radiometer instrument. *J. Atmos. Oceanic Technol.,* **15,** 697–707.

Gordon, H. R., J. W. Brown, and R. H. Evans, 1980: Exact Rayleigh scattering calculations for use with the NIMBUS-7 Coastal Zone Scanner. *Appl. Opt.,* **19,** 3427–3428.

Hansen, J. E., and L. D. Travis, 1974: Light scattering in planetary atmospheres. *Space Sci. Rev.,* **16,** 527–610.

Harrison, L., J. Michalsky, and J. Berndt, 1994: Automated multifilter rotation shadowband radiometer: An instrument for optical depth and radiation measurements. *Appl. Opt.,* **33,** 5188–5125.

Holben, B. N., and Coauthors, 1998: A federated instrument network and data archive for aerosol characterization. *Remote Sens. Environ.,* **66,** 1–16.

Kasten, F., and A. T. Young, 1989: Revised optical air mass tables and approximation formula. *Appl. Opt.,* **28,** 4735–4738.

Lenoble, J., 1993: *Atmospheric Radiative Transfer.* Deepak Publishing, 500 pp.

Morys, M. F., F. M. Mims III, and S. E. Anderson, 1996: Design, calibration and performance of MICROTOPS II hand-held ozonometer. *12th Int. Symp. on Photobiology,* Vienna, Austria, International Congress on Photobiology. [Available online at http://www.solar.com/ftp/papers/mtops.pdf.]

Paltridge, G. W., and C. M. R. Platt, 1976: *Radiative Processes in Meteorology and Climatology.* Elsevier Scientific, 318 pp.

Reagan, J. A., L. W. Thomason, B. M. Herman, and J. M. Palmer, 1986: Assesment of atmospheric limitations on the determination of the solar spectral constant from ground-based spectroradiometer measurements. *IEEE Trans. Geosci. Remote Sens.,* **GE-24,** 258–266.

Russell, P. B., and Coauthors, 1993: Pinatubo and pre-Pinatubo optical-depth spectra: Mauna Loa measurements, comparisons, inferred particle size distributions, radiative effects, and their relationship to lidar data. *J. Geophys. Res.,* **98,** 22 969–22 985.

Schmid, B., and C. Wehrli, 1995: Comparison of sun photometer calibration by use of the Langley technique and standard lamp. *Appl. Opt.,* **34,** 4500–4512

Shaw, G. E., 1982: Solar spectral irradiance and atmospheric transmission at Mauna Loa Observatory. *Appl. Opt.,* **21,** 2006–2011.

——, 1983: Sun photometry. *Bull. Amer. Meteor. Soc.,* **64,** 4–11.

Thomason, L. W., B. M. Herman, and J. A. Reagan, 1983: The effect of atmospheric attenuators with structured vertical distribution on air mass determinations and Langley plot analysis. *J. Atmos. Sci.,* **40,** 1851–1854.

Volz, F. E., 1959: Photometer mit Selen-photoement zurspektralen Messung der Sonnenstrahlung und zer Bestimmung der Wallenlangenabhangigkeit der Dunsttrubung (in German). *Arch. Meteor. Geophys. Bioklimatol.,* **B10,** 100–131.

——, 1974: Economical multispectral sun photometer for measurements of aerosol extinction from 0.44 μm to 1.6 μm and precipitable water. *Appl. Opt.,* **13,** 1732–1733.